Surge current protection for railway traction applications

Michael Gleissner, Mark-M. Bakran

UNIVERSITY OF BAYREUTH
DEPARTMENT OF MECHATRONICS
CENTER OF ENERGY TECHNOLOGY
Universitaetsstrasse 30
Bayreuth, Germany
Phone: +49 (0) 921-55 7804
Email: michael.gleissner@uni-bayreuth.de
URL: http://www.mechatronik.uni-bayreuth.de

Acknowledgments

This work was supported by the Federal Ministry for Economic Affairs and Climate Action on the basis of a decision by the German Bundestag.

Federal Ministry
for Economic Affairs
and Climate Action

Keywords

≪Over-current protection≫,≪Protection device≫, ≪Fault handling strategy≫,≪Faults≫, ≪Railway traction system≫, ≪Silicon Carbide (SiC)≫

Abstract

Reducing the transformer impedance for higher efficiency results also in a higher surge short-circuit current for railway traction applications. This paper addresses the problem of an I^2t-value higher than the nominal rating of SiC MOSFET body diodes. Circuit options for protecting the intact components after a single failure are presented and examined.

Introduction

In railway traction, by increasing the switching frequency of the input converter, it is possible to reduce the impedance of the transformer and thus to reduce losses. The free-wheeling diodes of the power modules must be designed for short-term, high current loads. If a switch in the four-quadrant input converter fails as a short-on or if the DC-link circuit is short-circuited, this leads to a high, mostly recurring surge current load on the still functioning diodes from the line via the transformer (see Fig. 1). Furthermore, in the event of an active bridge short-circuit of a B6 pulse-controlled inverter, the electrical machine can feed back, which also results in a high current load on the diodes. In the data sheets, the I^2t-value is usually specified by a sinusoidal current half-wave with a length of 10 ms, which the component can withstand as a maximum [1, 2]. The measurement of 10 ms results from half the period duration in the 50 Hz network. Since the AC railway supply network in Germany and other European countries operates at 16.7 Hz, the data sheet values must be evaluated accordingly. Since the diode is integrated in SiC MOSFETs, the additional module freewheeling diodes for normal operation can be saved. The requirements of surge current robustness are transferred to the body diodes. In the case of voltage classes below 3.3 kV or with Si technology, the components can handle the previously expected maximum surge current strengths of usually less than 1 MA^2 s [3, 4]. If their surge short-circuit current strength is not sufficient, appropriate protection concepts must be applied, which will be presented and discussed in this paper. As far as the authors are aware, there are no relevant and freely accessible references on this very specific topic of surge current protection for railway traction applications due to short-on failures.

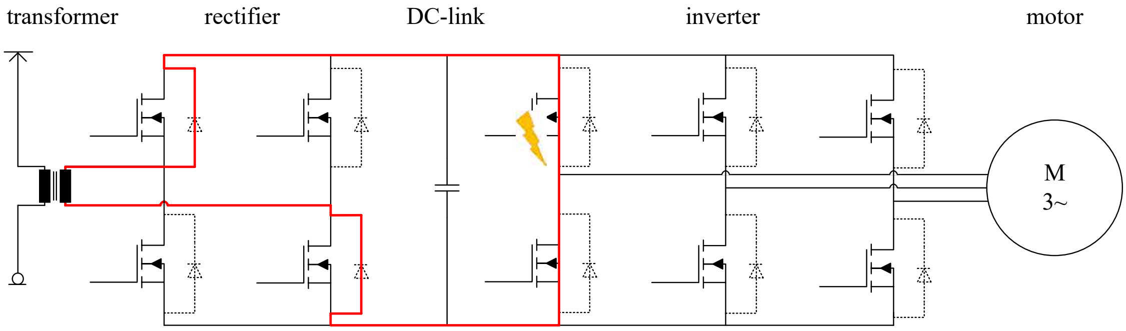

Fig. 1: Line-fed transformer, four-quadrant converter as rectifier, DC-link circuit, inverter and electrical machine. The dashed diodes indicate the body diodes of SiC-MOSFETs. Illustrated in red is a surge current due to a DC-link short-on failure. The body diodes within the current path have to be protected from secondary failure caused by a too large I^2t-value.

Basics on I^2t-value

The I^2t-value, which corresponds to the time integral of the squared current, is used to characterize the surge current robustness of components [5]:

$$I^2t = \int i^2(t)\mathrm{d}t \tag{1}$$

The equivalent circuit diagrams in Fig. 2 can be used to estimate the surge short-circuit current and I^2t-value for DC-link as well as single switch short-on failures. The transformer is represented by an ideal AC voltage source with transformer leakage inductance and transformer resistance. All sizes are related to the secondary side to which the four-quadrant converter is connected.

(a) DC-link short-on failure

(b) single switch short-on failure

Fig. 2: Simplified equivalent circuit diagrams for the line-side surge current

The related short-circuit voltage of the transformer depends on its leakage inductance and resistance. The lower the related short-circuit voltage, the lower the leakage inductance and resistance of the transformer. This in turn leads to a higher current in the event of a failure and thus I^2t-value. If the failure occurs in the voltage zero crossing, the worst case is obtained with the maximum amount of the current. If the fault occurs in a voltage maximum or voltage minimum, the best case results with the minimum amount of current. In the event of a single-chip short-on failure, the surge current can only flow in one direction and a mean value in the current that is dependent on the time of the failure cannot be reduced over several periods, as is the case with an DC-link circuit short-on. Therefore, in the event of a shutdown after several periods, a higher I^2t-value for the single-chip short-on failure results. The shape of the first period is identical for both failure scenarios. Fig. 3 shows the simulated voltage and current curves for DC-link and single chip short-on failure in the worst and best case as well as the associated I^2t-value. The failure occurs at time $t = 0\,\mathrm{s}$.

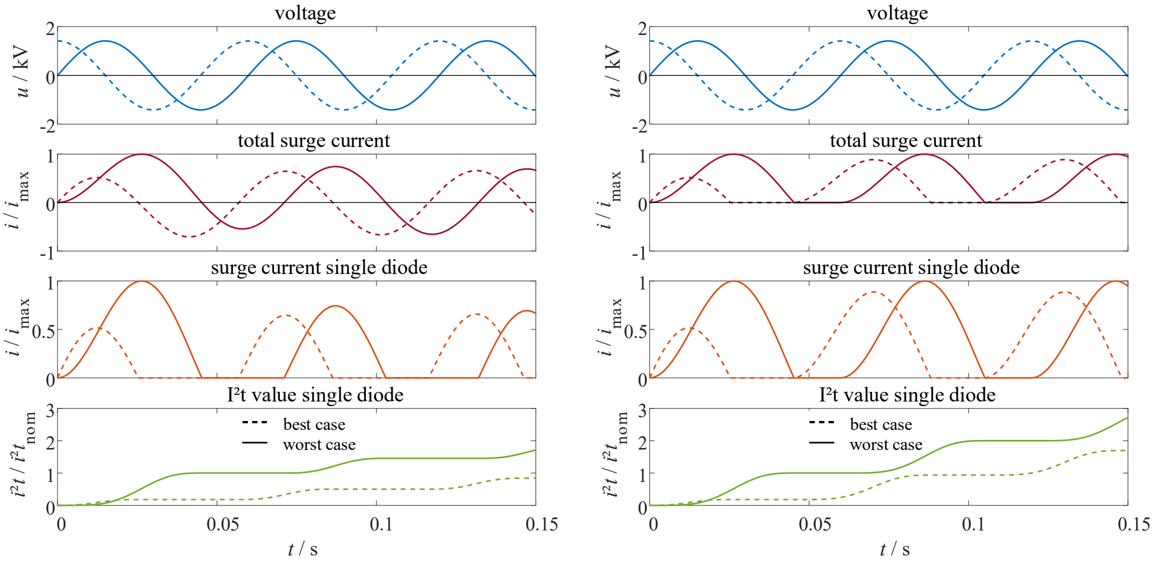

(a) DC-link short-on failure

(b) single chip short-on failure

Fig. 3: Simulated voltage and current curves in the worst and best case as well as the associated I^2t-value

Protective measures

Protective measures are necessary to minimize the stress of still healthy semiconductor devices within the surge current path, e.g. SiC MOSFET body diodes. Technical solutions can be based on switches, diodes or a combination of both. Their working principle and characteristics are given in the following subsections.

Mechanical circuit breaker

In previous applications, surge currents due to short-on failures are recognized by the central control unit and switched-off by opening the mechanical main switch on the primary side of the transformer in a time range of typically 60 to 80 ms, whereby the current can only be stopped after the subsequent zero current crossing due to an arc occurring [6] (see Fig. 4). With 16.7 Hz line frequency, this can be only after one or even two full sine half-waves depending on the failure scenario and time (best/worst case). The simulation results for the failure scenarios in the best and worst case vary from 3 to 20 $\mathrm{MA^2\,s}$. These I^2t-values are too large and better protection measures are required.

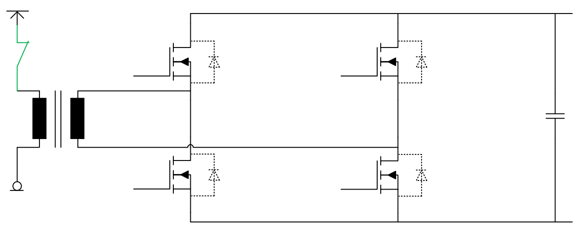

Fig. 4: Circuit breaker on AC-primary side (either mechanical or semiconductor based)

Fast circuit breaker

Instead of a mechanical disconnection switch, which requires at least a half-period to extinguish due to the arc, a faster switch can be used that can safely disconnect even during a current half-wave. Possible approaches to a solution result from electronic switches or from the use of pyro switches. Depending on the I^2t-robustness of the components, fast switches with a separation time below 10 ms are required.

Crow-bar

A crow-bar on the secondary side of the transformer can be used to relieve the rest of the circuit. A crow-bar typically consists of a thyristor, which enables after firing a bidirectional parallel path for the surge current. With a crow-bar, technically faster switching times are possible than with a disconnection element, e.g. 100 µs with a thyristor (see Fig. 5a). This is more than sufficient, because the same tripping times as with a fast disconnector are necessary to avoid a too large I^2t-value.

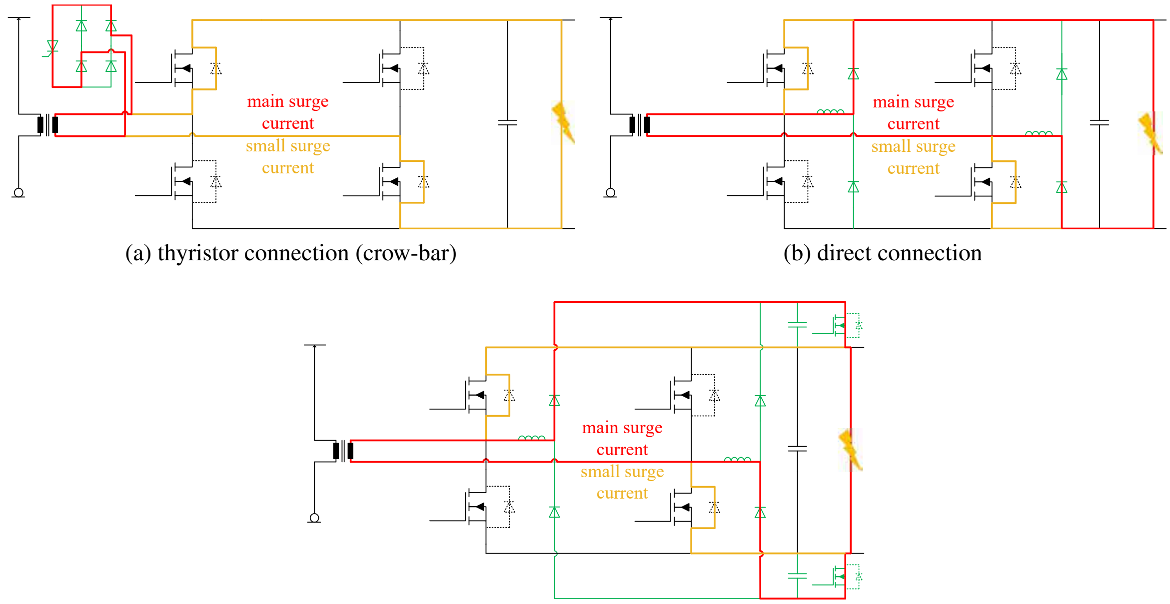

(a) thyristor connection (crow-bar)

(b) direct connection

(c) decoupling capacitors with low voltage MOSFET bridge

Fig. 5: Connection of paralleled Si rectifier diodes (marked in green) for surge short-circuit current relief after DC-link short-on failure

Paralleled Si rectifier diodes

Silicone rectifier diodes connected in parallel offer another option for reducing the surge short-circuit current stress. Their I^2t-robustness is typically in the range of 5 to 10 MA^2 s. They must be connected anti-parallel to the SiC MOSFETs in order to reduce the flow of current via the internal body diode of the SiC MOSFETs in the event of a failure, thereby relieving them and protecting them from destruction. Depending on the distance between the connection, a parasitic connection inductance arises, which can also be intentionally increased in order to influence the current distribution between Si rectifier diodes and SiC MOSFET body diodes. In normal operation, the Si diodes should only carry a small amount of current or no current at all in order to generate little or no switching losses. In the event of a surge current failure, however, they should take on as much current as possible. The variant of the direct connection is shown in Fig. 5b. A prerequisite for a successful implementation of this direct connection without additional switches is that the Si diodes have only very low reverse recovery loss. The variant of the diode activation by means of a thyristor is shown in Fig. 5a. The thyristor is activated in the event of a failure and thereby switches on the parallel Si rectifier diodes. These are switched-off in normal operation and cannot carry any current and thus cause no or only little loss. The thyristor must be designed for the full system voltage. It is a large and expensive component. Instead of the thyristor, the Si diodes can also be decoupled by capacitors during normal operation. In the event of a failure, these decoupling capacitors are bypassed by low-voltage MOSFETs and in this way switch-on the Si rectifier diodes (see Fig. 5c). For this circuit, it must be clarified which capacity the decoupling capacitors must have, what voltage they must be pre-charged to and how many low-voltage MOSFETs must be connected in parallel in order to be able to safely carry the entire surge short-circuit current in the event of a worst-case failure.

Analysis of paralleled Si rectifier diodes

Reverse recovery characteristic

In order to test the use of the direct connection, the reverse recovery behavior of a Si rectifier diode has been measured with a double-pulse circuit. The results in Fig. 6 indicate that even a very small load current of a few amperes leads to a very large reverse current peak. With a system voltage of 1.8 kV and a switching frequency of 3 kHz, this is associated with unacceptable losses. Therefore, the variant of the direct connection of the Si rectifier diodes is not further considered.

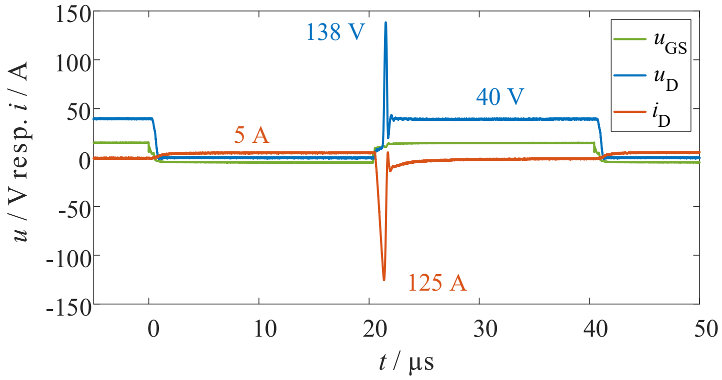

Fig. 6: Measurement of large reverse recovery peak even at low load current and low blocking voltage of diode DZ1070N22K

Loss due to $\mathrm{d}u/\mathrm{d}t$-stress

If the Si rectifier diodes are connected by the circuits shown in Fig. 5a and Fig. 5c, there are no reverse recovery losses because the diodes do not conduct during normal operation, but they still see a $\mathrm{d}u/\mathrm{d}t$ stress from the SiC MOSFETs which operate in parallel. The gradient of the voltage when switching can be adjusted using the gate resistance. The measured voltage at the diode and the capacitive charge reversal can be seen in Fig. 7 for various voltage slopes. The peak value of the capacitive recharging current increases linearly with the voltage gradient and results in a capacitance of the Si diode of about 2 nF. This capacitive recharging current leads to a power loss of about 10 W at a switching frequency of 3 kHz and a system voltage of 1.8 kV. This power loss is acceptable.

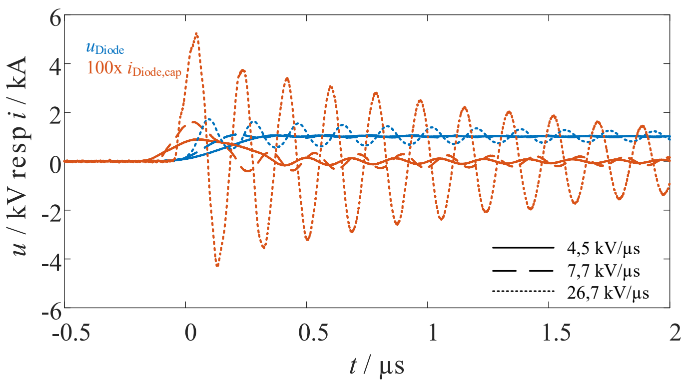

Fig. 7: Measurement of $\mathrm{d}u/\mathrm{d}t$ test for capacitance determination of Si diode DZ1070N22K

Peak rectifier characteristic of diode types

The diodes have to be decoupled during normal operation to avoid loss. The characteristic of Si diodes and fast diodes in a peak rectifier circuit has been tested with the circuit shown in Fig. 8a. The measured voltages after turn-on of S_1 and S_4 are shown in Fig. 8 for a fast diode and a Si diode. With the fast diode, the phase voltage u_{out} is below the capacitor voltage u_C after the switching process, which means that the diode is not conducting. The initial capacitor voltage is increased. The Si diode shows a voltage u_{out}, with is equal or above to the capacitor voltage and thus results in a conducting mode. The initial capacitor voltage is not increased and results in repetitive conduction mode of the Si diode and thus unwanted reverse recovery loss. But the fast diode has unfortunately only a small I^2t-robustness and cannot be employed for surge current release. Consequently, the Si diodes have to be decoupled by capacitors, which are actively charged to a voltage higher than the peak system voltage in order to avoid loss.

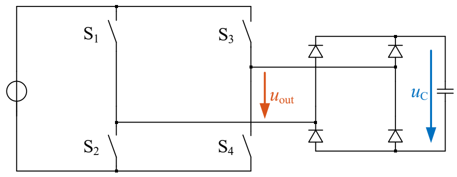

(a) Test circuit

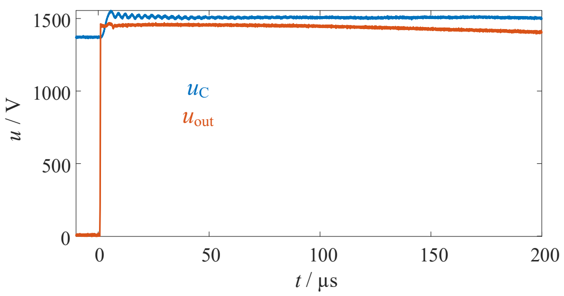

(b) Measurement with fast diode

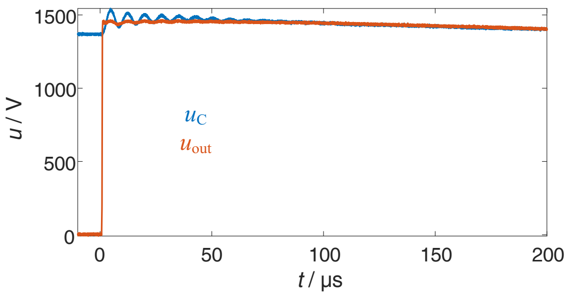

(c) Measurement with Si diode

Fig. 8: Peak rectifier test to check decoupling of diodes. Initially all switches are turned-off. S_1 and S_4 are turned-on at $t = 0$ s.

Design of decoupling capacitor

For the protection circuit depicted in Fig. 5c, the starting voltage and capacitance of the decoupling capacitor as well as the connection inductance must be dimensioned appropriately. As a first test, the measurement setup shown in Fig. 9a was implemented. The starting voltage of the capacitor is particularly relevant, which must be sufficiently high so that the Si diode does not conduct and thus does not cause any reverse recovery losses. In the first test, the Si rectifier diode and SiC MOSFETs are not yet properly scaled to one another. In addition, this test has not yet been carried out at a system voltage of 1.8 kV, but only at 100 V for a first function test. The measurement results of the decoupling circuit show that the Si rectifier diode conducts and causes reverse recovery if the capacitor is not charged or is insufficiently charged (see Fig. 9b). From a starting voltage of the capacitor of 9 V, the diode no longer conducts and you can only see the capacitive recharging current (see Fig. 9c).
This capacitive charge reversal current continues to charge the capacitor for each switching process. It is therefore necessary to provide a charging / discharging circuit for the decoupling capacitors, which precharges them sufficiently when the system is started up and continuously discharges them again during operation in order to keep the voltage stable.
Low-voltage MOSFETs in the voltage class of 100 V or less can be used as bypass switches in the event of a failure.

Surge current robustness of bypass low-voltage MOSFETs

The surge current robustness of single low-voltage MOSFETs in PG-HSOF-8 package has been investigated by means of destruction tests with the surge current test circuit shown in Fig. 10. The period and amplitude of the surge current can be adjusted by L_{surge}, C_{surge} and the initial voltage. Switch T_1 decouples and protects the voltage source and switch T_2 triggers the surge current sine half-wave. The diodes block the negative half-wave and thus prevent an oscillation. In case of an open-circuit failure of the DUT several serial connected diodes enable an additional current path. It should be noted that the total

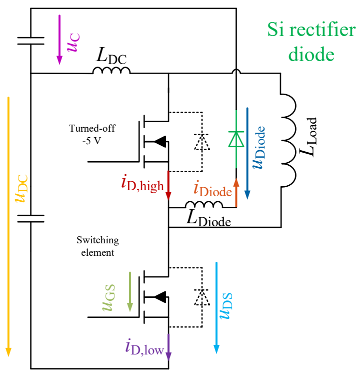

(a) measurement setup

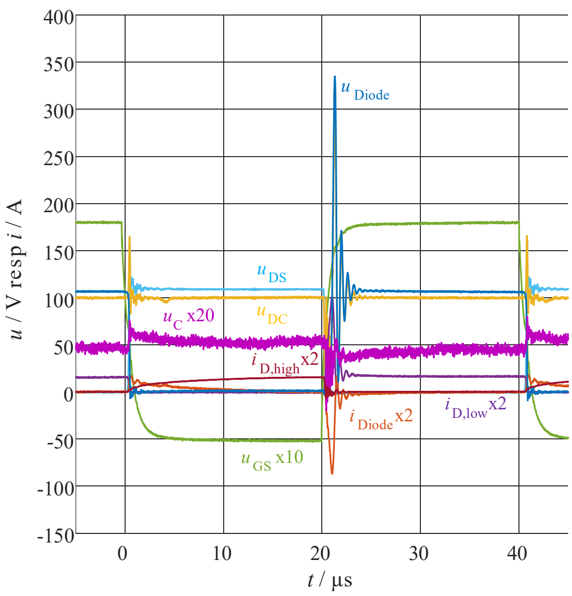

(b) 2.4 V starting voltage of capacitor - reverse recovery peak

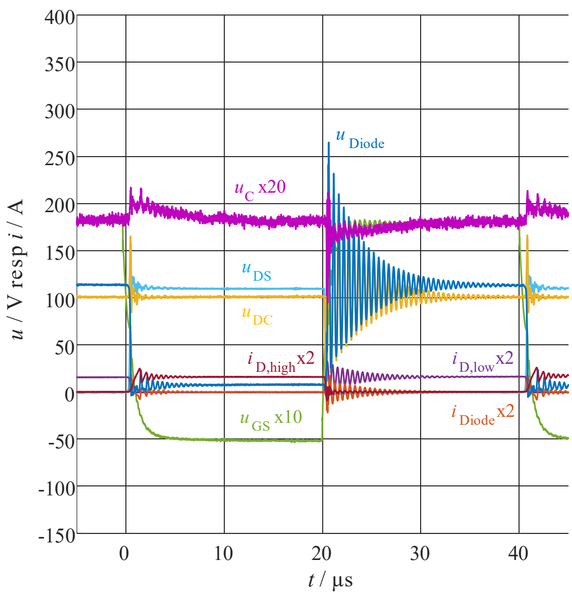

(c) 9.2 V starting voltage of capacitor - no reverse recovery peak

Fig. 9: Low voltage test of required pre-voltage u_C of capacitor to decouple Si rectifier diode

resistance of the circuit is less than the resistance for the damping case of the LCR series connection, so that a half-sine-wave oscillation is still produced. In particular, for longer durations of the half-sine oscillation in the range of 40 ms, the structure must have a very low resistance.

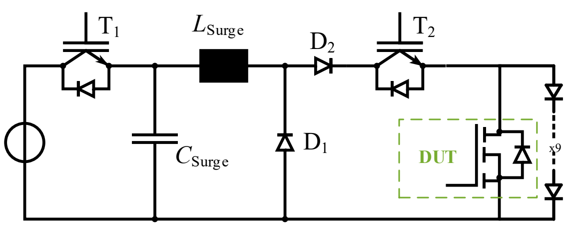

(a) Equivalent circuit

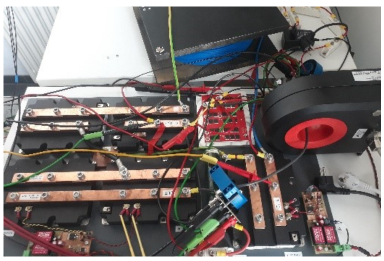

(b) Hardware setup

Fig. 10: Surge current test circuit

The last measurement before failure and the failure measurement are shown in Fig. 11. The failure limit of a single device is roughly at a peak current of just under 700 A. The tested switches have failed with low resistance in relation to the drain-source path, which is advantageous for later use as a bypass in the event of a failure.

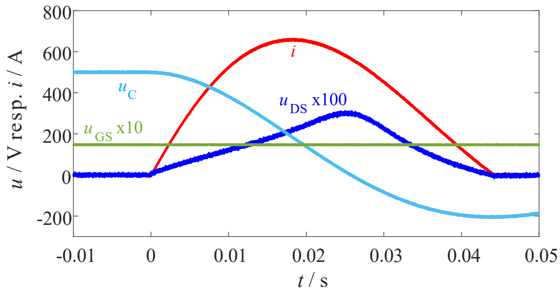

(a) Last good before failure

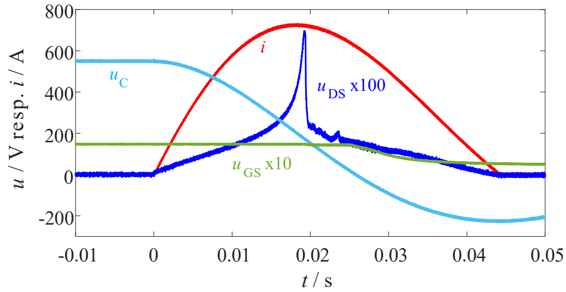

(b) Failure

Fig. 11: Surge current test measurement for single low-voltage MOSFET

The measured power loss was corrected by the circuit board resistance to get the power loss of the chip. This power loss has been applied to a thermal network in a simulation model, which corresponds to the data sheet value for the thermal impedance from junction to ambient. The failure temperature is in the range above 600 °C.

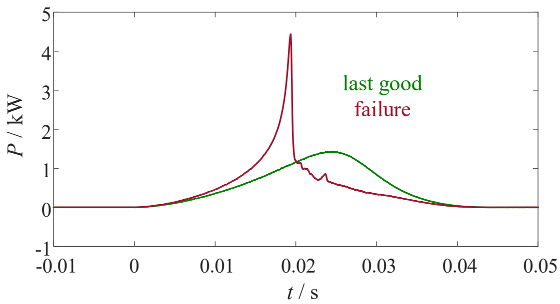

(a) measured power

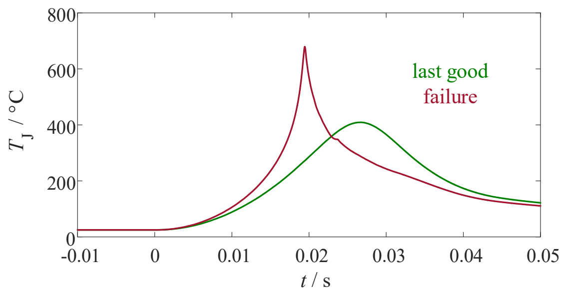

(b) simulated temperature

Fig. 12: Calculated power based on measurement and simulated junction temperature based on data sheet thermal impedance for last good and failure measurement

The permissible individual load results in around less than 50 low-voltage MOSFETs to be switched in parallel in order to reach sufficient surge current capability. To evaluate the effects when several dozens of MOSFETs are paralleled, a sample board (see Fig. 13) was designed and exposed to a surge current pulse with a peak value of 14 kA. The resistance of the paralleled MOSFETs on the board including contacts is less than 200 µΩ.

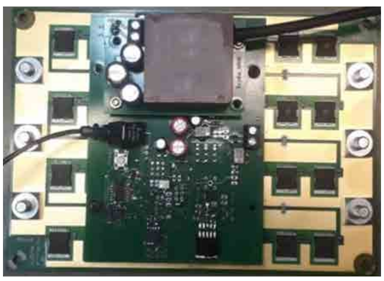

(a) Hardware setup

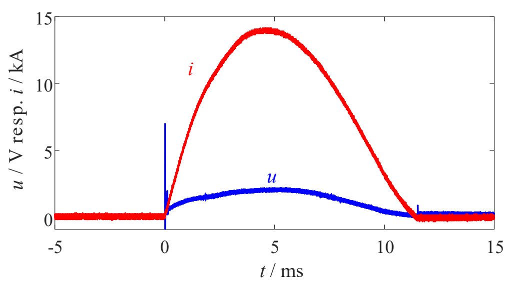

(b) Measurement of large surge current

Fig. 13: Low-voltage bypass switch consisting of several paralleled low-voltage MOSFETs

Conclusion

Simple simulation models were used to estimate which I^2t-values can be expected and which remedial measures appear sensible for the surge current in railway traction applications after short-on failures. Mechanical switches are not sufficient for a faster disconnection of the line side current. To limit the I^2t-value in the event of a failure, electronic or pyro switches with a separation time of below 10 ms are required. The use of a crow-bar directly at the input of the converter with thyristors also enables fast switching times and can achieve low enough I^2t-values. By connecting Si rectifier diodes with a high current carrying capacity in parallel with the SiC MOSFETs, according to the simulation, sufficient relief can be achieved in the event of a failure. A direct connection is not possible due to the reverse recovery losses of the Si diodes. The voltage slope load of the Si diodes, both with the connection by means of a thyristor and the low voltage decoupling capacitor circuit, is acceptable. The decoupling capacitors have to be charged to a voltage level higher than 9 V so that the Si diodes are decoupled during normal operation. In the event of a failure, these can be bypassed, for example, by a sufficient number of paralleled low-voltage MOSFETs. This represents an alternative to the previously known solution using a thyristor as an activation element. A prove of concept implementation of the solution was successfully exposed to a large surge current.

References

[1] P. Hofstetter and M.-M. Bakran, "Comparison of the Surge Current Ruggedness between the Body Diode of SiC MOSFETs and Si Diodes for IGBT," in *CIPS 2018; 10th International Conference on Integrated Power Electronics Systems*, 2018.

[2] ——, "Predicting Failure of SiC MOSFETs under Short Circuit and Surge Current Conditions with a Single Thermal Model," in *Proceedings of the 20th European Conference on Power Electronics and Applications (EPE ECCE Europe)*, 2018.

[3] F. Carastro, J. Mari, T. Zoels, B. Rowden, P. Losee, and L. Stevanovic, "Investigation on diode surge forward current ruggedness of Si and SiC power modules," in *Proceedings of the 18th European Conference on Power Electronics and Applications (EPE ECCE Europe)*, 2016.

[4] Z. Dong, R. Ren, F. Wang, Z. Dong, R. Ren, and F. Wang, "Evaluate I2t Capability of SiC MOSFETs in Solid State Circuit Breaker Applications," in *IEEE Energy Conversion Congress*, 2020, pp. 6043–6048.

[5] R. H. Kaufmann, "The Magic of I2t," *IEEE Transactions on Industry and General Applications*, vol. IGA-2, no. 5, pp. 384–392, 1966.

[6] M.-M. Bakran, H.-G. Eckel, M. Helsper, and A. Nagel, "Next generation of IGBT-modules applied to high-power traction," in *Proceedings of the 12th European Conference on Power Electronics and Applications (EPE ECCE Europe)*, 2007.